

1. Surveys and Survey Interpretation

Long-Wavelength Aeromagnetic Anomalies and Deep Crustal Magnetization in Manitoba and Northwestern Ontario, Canada*

D. H. Hall

Geophysics Section, Department of Earth Sciences,
University of Manitoba, Winnipeg, Canada

Received March 12, 1974; Revised Version May 22, 1974

Abstract. A new type of aeromagnetic anomaly map (a long-wavelength anomaly map with anomaly widths in the range 60 km. $< \lambda < 4000$ km) is presented for the area. It is believed that this group of anomalies represents a physically distinct field. This field shows considerable correlation with the broad features of deep crustal structure as derived from seismic sounding; linear relationships were found between the field and depths to the bottom of the crust and to the boundary between the upper and the lower crustal layers, as well as to the thickness of the lower crustal layer. A theoretical relationship connecting structure on magnetized layers to magnetic anomalies is given showing that the linear relationships are to be expected. It is shown that the lower crustal layer is the most likely source of the anomalies, with an intensity of magnetization of 5.3×10^{-3} emu/cc. It is also indicated that the upper crustal layer could also be the source, but that a shallow plate of magnetization could not explain the anomalies. Thus *deep crustal magnetization* must (on all interpretations made in the present paper), be responsible for the long-wavelength anomalies. Also, these anomalies are strongly related to major features in surface geology.

Key words: Long-Wavelength Aeromagnetic Anomalies — Deep Crustal Magnetization — Canadian Shield.

Note

In order to facilitate comparison with existing publications on magnetizations of rocks and with existing magnetic anomaly maps, e.m. units are used for magnetization, and gammas for field strengths.

(1 gamma = 1 nanotesla, and $I_{STU} = 4\pi I_{emu}$)

* Paper presented at IAGA second scientific conference, Kyoto, September 1973.

Paper No. 3, Centre for Precambrian Studies, University of Manitoba.

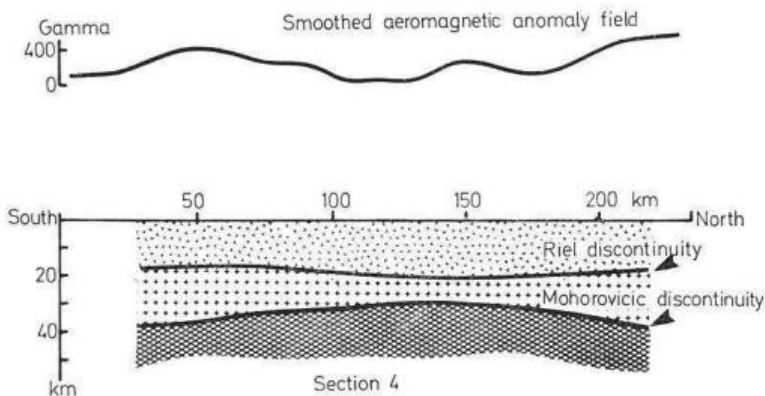


Fig. 1. Crustal section no. 4 (Fig. 3), with regional anomaly field along the corresponding line on Fig. 1 (1 gamma = 1 nanotesla)

Introduction

Regional Magnetic Anomalies

Compilation maps of aeromagnetic anomalies in the wavelength (anomaly width) band $\lambda > 20$ km. have proven to be of value in studies of magnetic units lying in the upper layer of the earth's crust, to depths of approximately 20 km. In northwestern Ontario and Manitoba, such maps have been constructed and interpreted by Bhattacharyya and Morley (1965), by Hall (1968a), by McGrath and Hall (1969), by Hall (1971), and by Coles (1973).

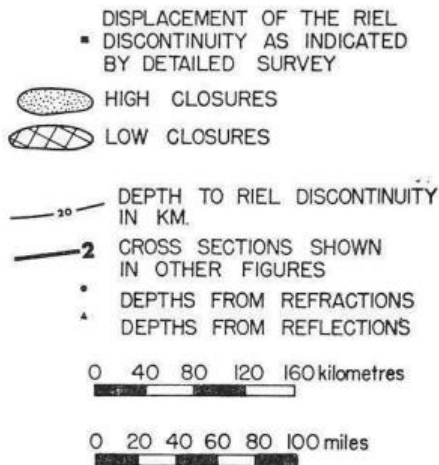
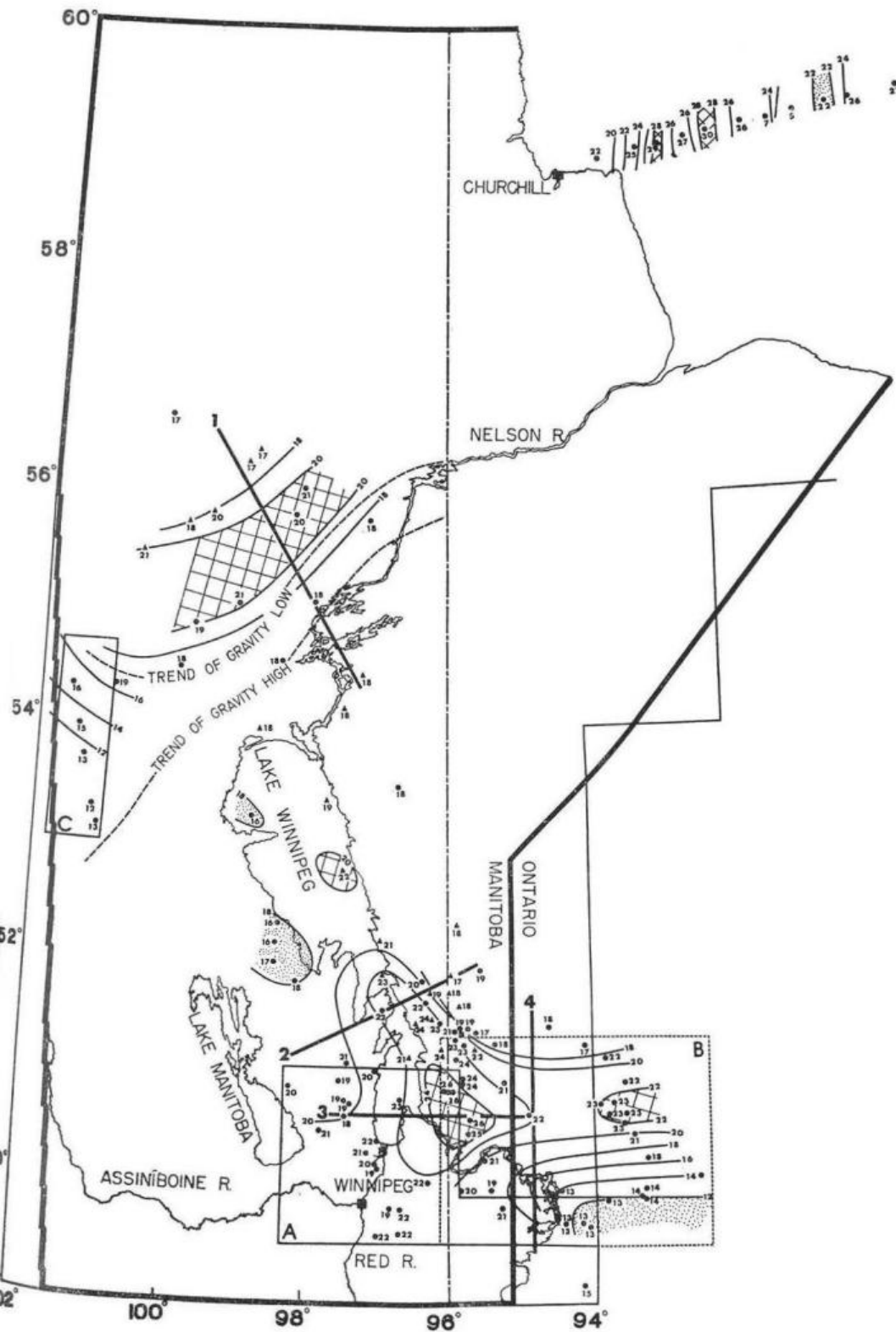


Fig. 2 Depth to Riel discontinuity (boundary between upper and lower crustal layers) (from Hall and Hajnal, 1973)





A similar map has been prepared for the British Isles (Hall and Dagley, 1970). The first three of the references mentioned above represent successive stages in the preparation of a map of aeromagnetic anomalies in the band $\lambda > 20$ km. for the area. This map has recently been updated and is to be published by the Manitoba Mines Branch as a map (Hall, McGrath and Richards, 1974). This map, as indicated by its wavelength band, portrays a filtered (or smoothed) compilation of aeromagnetic maps with anomalies of width less than 20 km. removed by the filtering process. In the aforementioned publications, these maps are referred to as "regional anomaly maps".

The most prominent features seen on visual examination of the regional anomaly maps are anomalies and anomaly trends with widths measuring some tens of kilometers. In addition, however, somewhat larger areas with general levels of magnetic field differing one from the other can be seen on them. The Ontario-Manitoba maps quoted above are examples. The anomalies and anomaly trends group themselves into alternating belts of high and low field crossing the area. Wilson (1971) noted these groupings and attributed them to the effects of a system of crustal blocks, which differ in magnetic properties. The individual smaller wavelength anomalies determine the general character of the map while the grouping into belts is present as a more subtle effect. The question arises as to the possibility that the latter represents a physically distinct field of longer wavelength underlying the high-amplitude, narrow anomalies. Such underlying long-wavelength fields have been mapped in various parts of the world. Zietz *et al.* (1970) found that a field in the band $200 \text{ km} < \lambda < 2000 \text{ km}$ lies over the United States. Regan (1974) has extended this work on a worldwide basis.

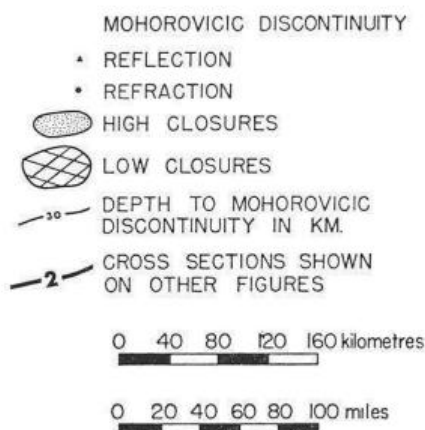


Fig. 3 Depth to Mohorovicic discontinuity (from Hall and Hajnal, 1973)

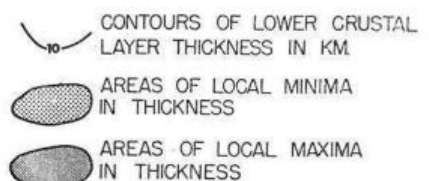
Possible Long-Wave Length Components of Regional Anomaly Maps in Manitoba and Northwestern Ontario

Crustal seismic surveys have indicated a two-layer structure for the earth's crust in these areas. The upper layer bottoms at a seismic discontinuity which has been named locally "the Riel discontinuity". Maps of the Riel (*R*) and Mohorovicic (*M*) discontinuities have been published, covering a strip 1000 km long and 300 km wide in Manitoba and northwestern Ontario (Hall and Hajnal, 1973). These maps are reproduced in the present paper in Figs. 2 and 3. During comparison of these maps with other geophysical data certain long-wavelength components ($\lambda > 100$ km) were distinguished underlying the regional magnetic anomaly field. These components appeared to be correlated with structural features of the *R* and *M* discontinuities. It was suggested that the thicknesses of the crustal layers are somehow related to these long-wavelength anomalies (Hall and Hajnal, 1973, p. 903, and Fig. 1, this paper). Attempts were therefore made to extract the long-wavelength components from the regional anomaly maps and to follow up the suggestion that they might be somehow connected with crustal structure. The present paper gives the results of these studies.

The Long-Wavelength Anomaly Map

Choice of Cutoff Wavelength

The anomaly map in the present paper has a cutoff wavelength of 60 km. This value was chosen for two reasons. First, the shortest wavelength anomalies from the Riel and Mohorovicic discontinuities for a layered



0 40 80 120 160 kilometres



0 20 40 60 80 100 miles


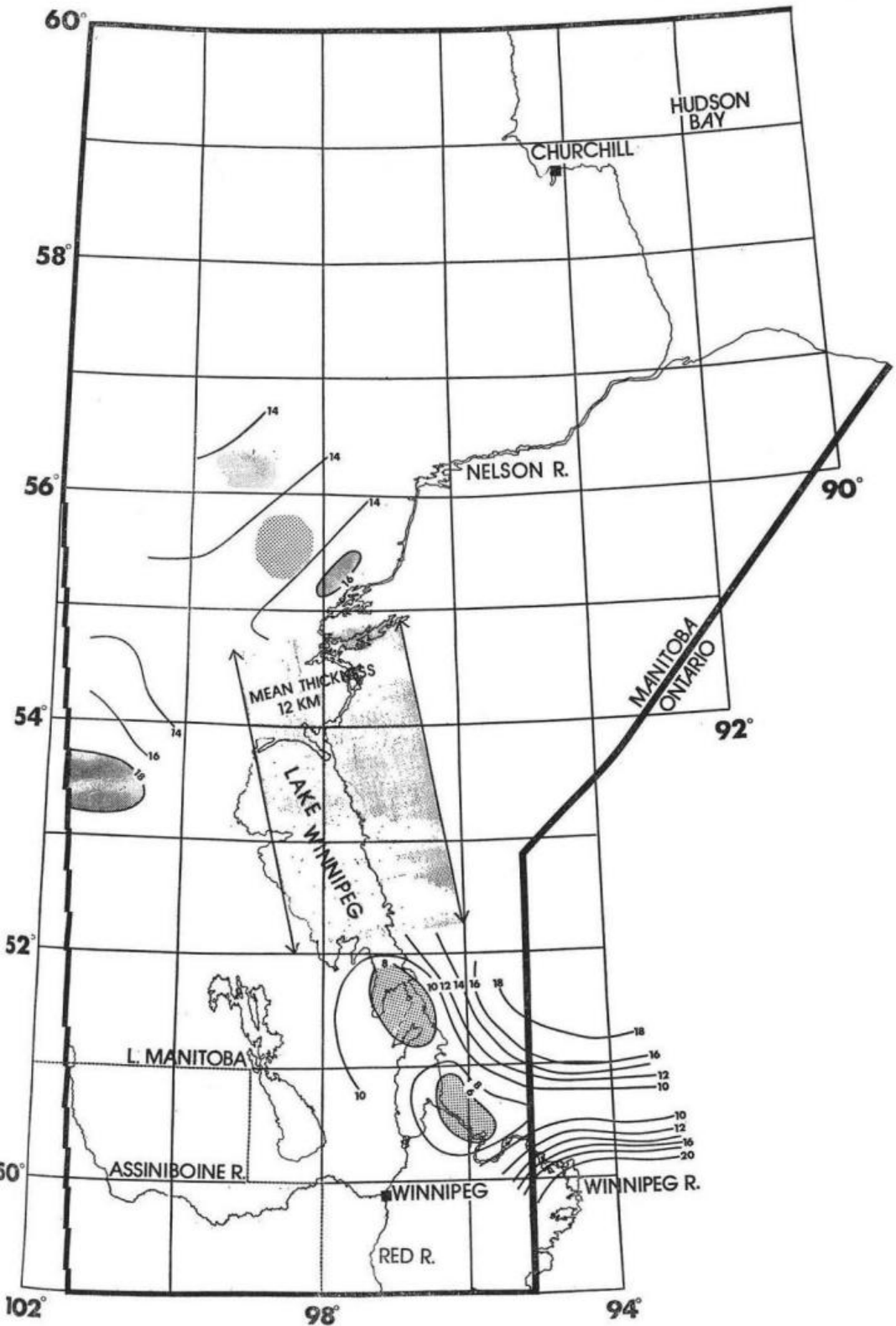



Fig. 4 Thickness of lower crustal layer



magnetic model might reasonably be expected to be due to fault displacements. On calculation, such structures would yield wavelengths in the 50–60 km range. The map then represents a bandpass which would contain the physically distinct field due to layer-like crustal magnetization, if it exists. Secondly, existing data (at 3-km spacing) decimated to give a grid of data points with 9 km. spacing yields, on filtering with the operator developed by McGrath and Hall (1969), a cutoff wavelength of 60 km. This cutoff, then, is physically realistic and was computationally simple to obtain given the data and the computational methods available. Removal of the core-generated fields yields a bandpass of $60 \text{ km} < \lambda < 4000 \text{ km}$. The core-generated fields were approximated by fitting a second-order surface (over the area of Fig. 5) to the Dominion Observatories Branch (1965) map of total field, and subtracting this best-fit field from the smoothed data.

Interpretation of Long-Wavelength Anomalies

It is an observed fact (evident from visual comparison of Figs. 2, 3, 4 and 5) that the long-wavelength anomalies exhibit a close correlation with deep crustal structure as derived from seismic surveys. One possibility suggested by this fact is that the magnetic sources for this field lie deep within the crust, with their distribution controlled by broad crustal structure. Two extreme models for such deep magnetization can be constructed. The first consists of uniformly magnetized layers bounded by the *R* or the *M* discontinuity (or both). The second consists of lateral inhomogeneities in magnetization within either of the crustal layers, or below the

LONG - WAVELENGTH REGIONAL ANOMALIES

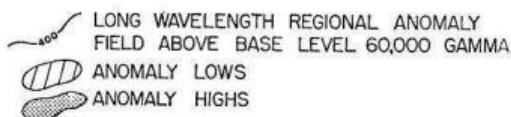
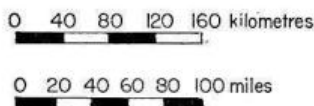
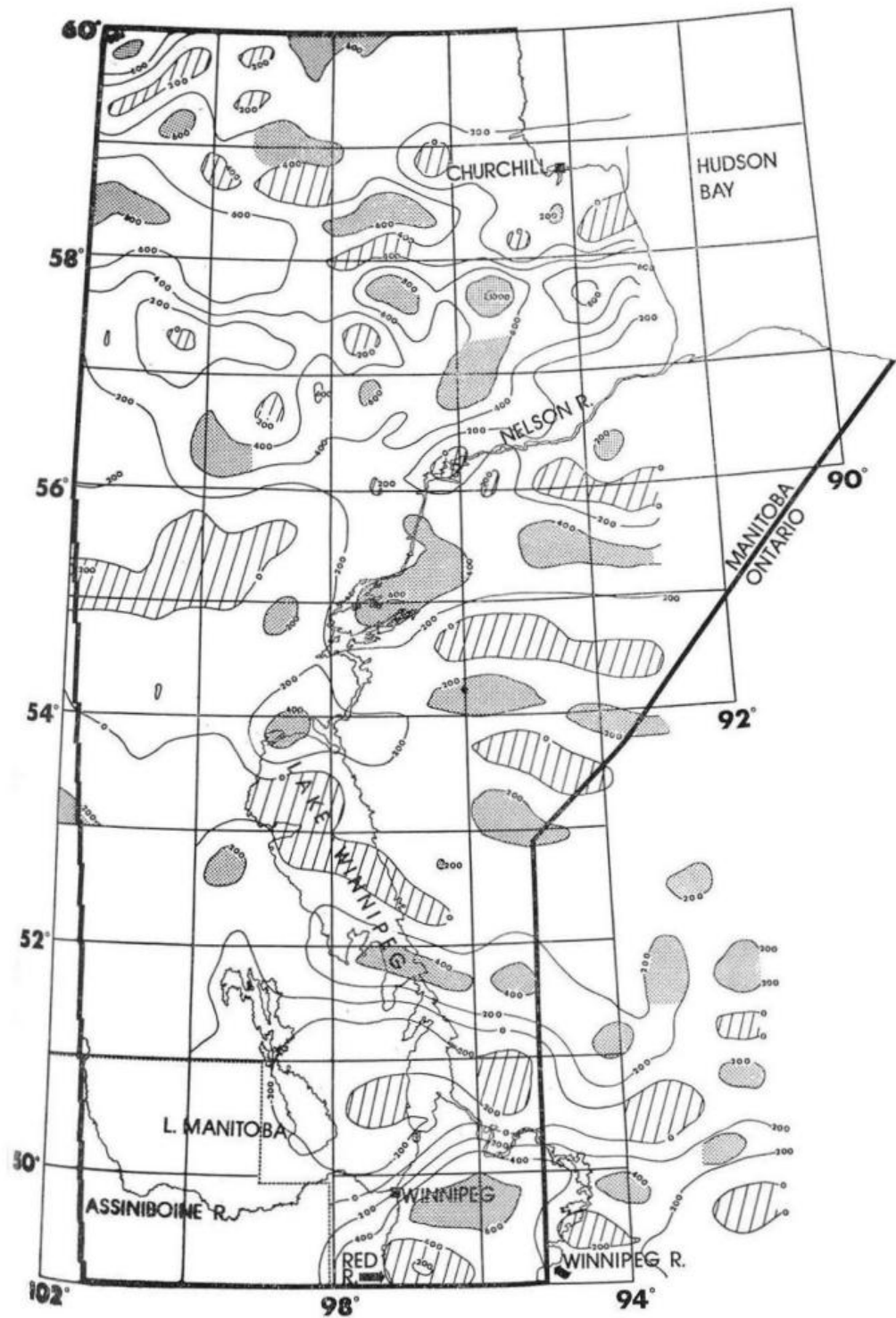


Fig. 5 Long-wavelength magnetic anomaly field ($60 \text{ km} < \lambda < 4000 \text{ km}$) in gammas above a best-fit second order surface to the core-generated field. (1 gamma = 1 nanotesla)





crust. Such lateral inhomogeneities could also, in many cases, match the broad dimensions of crustal structure because of the following considerations.

As shown in Fig. 6, the long-wavelength anomaly map and the seismic interfaces can be divided into a number of zones. These zones, furthermore, mark out definite geological units as mapped at the surface. The deep crustal structure is clearly reflected in surface geology. This relationship is convincingly discussed by Wilson (1971), in proposing a block structure for the Superior province of the Canadian Shield. Thus even though the seismic boundaries of Figs. 2 and 3 are continuous over the whole area, the crustal layers bounded by them could have quite different compositions in different parts of the area, corresponding to the system of geological units mentioned above. If this is so, and if the various compositions affect magnetization markedly, then there would be lateral inhomogeneities in magnetization, with wavelengths comparable to those of crustal structures. These lateral inhomogeneities, even if the magnetic units corresponding to them extended to a uniform depth, could then cause anomalies having similar widths to those of structures on crustal interfaces. The corresponding anomalies would be very difficult to separate from those due to boundaries of uniformly magnetized layers. Further complications could occur if lateral inhomogeneities and undulating boundaries both acted to determine the anomalies.

Situations of this type are, of course, often met with in anomaly interpretation as part of the "ambiguity problem". The most an interpreter can do, in the absence of additional information, is to bear ambiguity in mind and begin exploring the implications of the various possible models.

There is one further implication of the connection between deep crustal structure and regional geology at the surface which should be mentioned. Thin plates of magnetization near the surface, controlled in width by deep

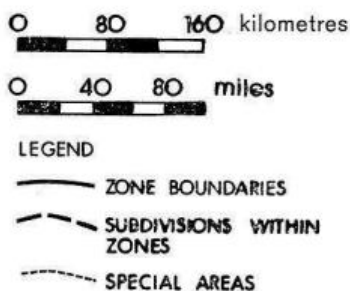


Fig. 6 Zones over which fields and depths to the crustal boundaries were averaged for Table 1



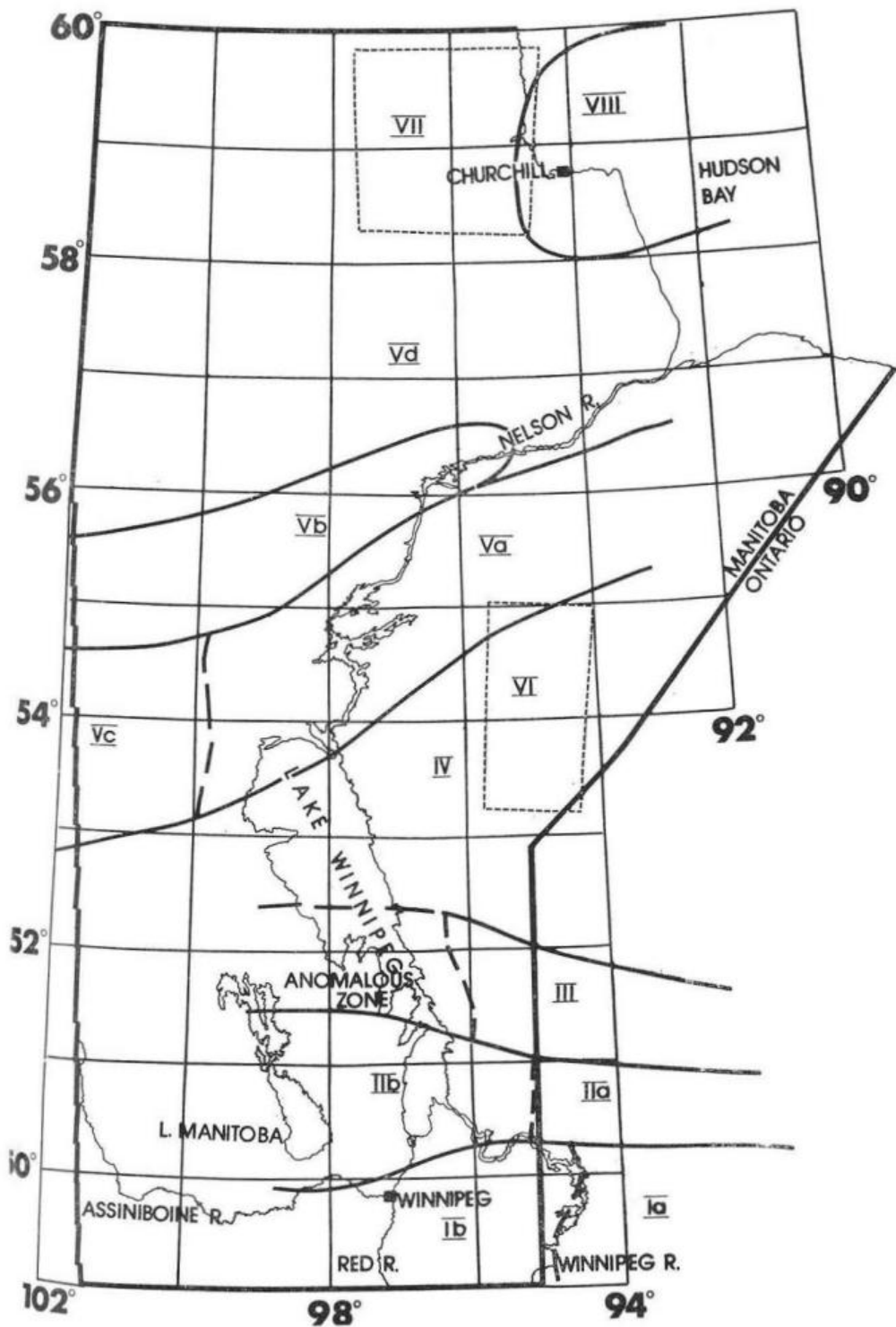


Table 1

Zone	$F(\gamma)$	$M(\text{km})$	$R(\text{km})$	$LL(\text{km})$	$t(\text{km})$	
I	425	38	13	25	18	Kenora Block ^a
IIa	0	32	21	11	1	} English River Block ^a
IIb	-200	31	22	9	-2	
III	250	34	18	16	7	Red Lake Block ^a
IV	125	30	18	12	3	Area of uniform crustal structure
Va	200	33	18	15	6	Structure in the vicinity of the Nelson River (Thompson) lineament
Vb	10	34	20	14	4	
Vc	60	31	15	16	8	
Vd	250	34	18	16	7	Area to north and west of the Nelson River (Thompson) lineament
VI	150	31	-	-	-	} Special areas
VII	500	40	-	-	-	
VIII	200	43	27	16	3	West-central Hudson Bay

^a Fault blocks of the western Superior Province as defined by Wilson (1971, p. 41). These are components of a proposed aulacogen structure (Hall and Hajnal, 1969, 1973). The "lower layer parameter" is given by $t = M - 1.5R$ for the area under study.

crustal structure, could conceivably cause long-wavelength anomalies, without requiring deep magnetization at all. Tests of this suggestion will be the subject of a later section.

Let us now begin to examine the suggested models. Leaving the suggestion of a near-surface plate of magnetization aside for the moment, let us compare the two extreme models of deep crustal magnetization: uniformly magnetized crustal layers, and lateral inhomogeneities. Both imply deep crustal magnetization, but the manner of its occurrence is very different in the two cases, with different implications in each for crustal evolution. Therefore, it is important to evaluate them both. Let us begin with the model suggesting uniformly magnetized crustal layers.

A Method of Comparing Crustal Structure and Long-Wavelength Anomalies

Comparison among Figs. 2, 3, 4, and 5 indicate 12 zones (shown on Fig. 6), in each of which crustal structure and magnetic field are relatively uniform, and significantly different from the corresponding quantities in

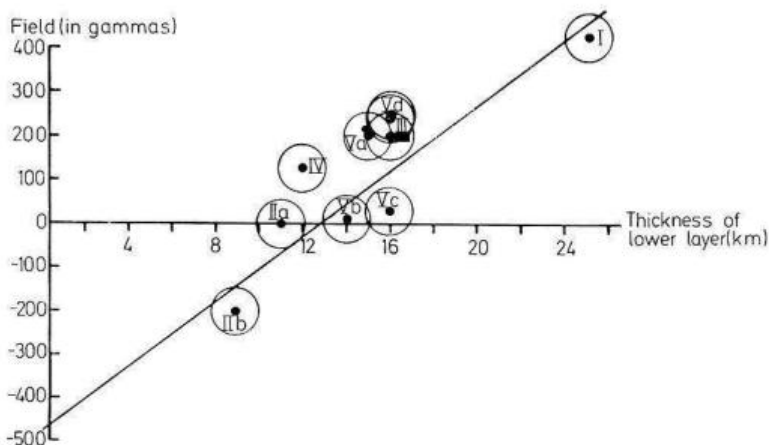


Fig. 7. Plot of field against thickness of lower layer, from values in Table 1 (1 gamma = 1 nanotesla)

neighbouring zones. In Table 1 the average values of field (F), total crustal thickness (M), upper-layer thickness (R), and lower-layer thickness (LL) for these zones are summarized. For the area covered by all of these data (comprising zones I to V) the values in Table 1 were obtained by simple averaging over the zones. Zones VI and VII are special areas, over which the long-wavelength anomaly data extend, but for which coverage with detailed crustal seismic surveys is not available. Data on crustal thickness are, however, available for these two zones from a line of data recorded by Mereu and Hunter (1969) (and compiled and compared with Figs. 2 and 3 by Hall (1971, p. 84)), and provide the values given in Table 1. Zone VIII covers a portion of west-central Hudson Bay. Magnetic data are taken from Fig. 5, as well as from the Aeromagnetic Map of Canada (Morley and MacLaren, 1967). Seismic information is taken from the papers of Hajnal (1968) and Hall (1968b). These zones for the most part represent geologically distinct features, the significance of which will be discussed in a later section.

Let us now examine these figures to see if they give any indications as to whether the model under examination in the present section (uniformly magnetized layers with intensity contrasts along or conformable with the crustal seismic discontinuities) applies in the area. An interesting relationship among F , LL , R and M emerges when plots of F against the others (as shown in Figs. 7, 8, 9 and 10) are made. The circles represent a reasonable estimate of uncertainty in the parameters plotted. Considering that a certain amount of scatter may be expected due to the influence of intensity inhomogeneities, which almost certainly exist within the crust, it is not unreasonable to suggest that linear relationships hold in these three figures. Regardless

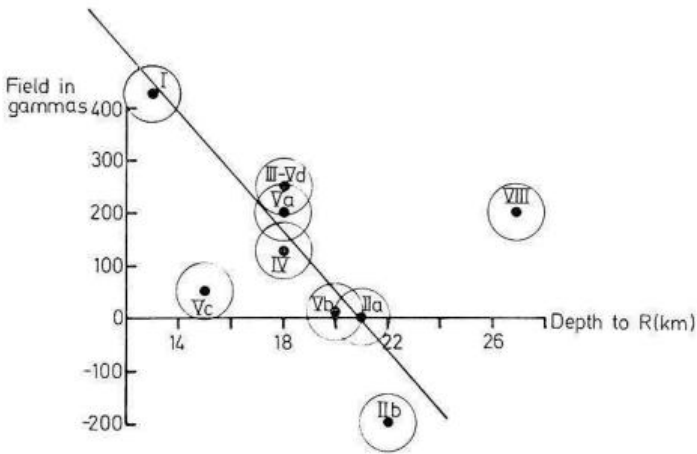


Fig. 8. Plot of field against thickness of upper crustal layer, from values in Table 1 (1 gamma = 1 nanotesla)

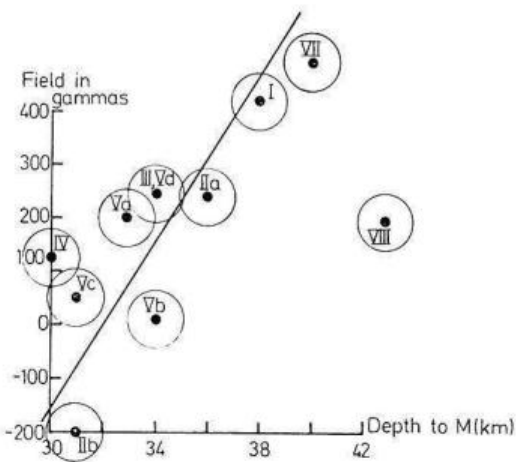


Fig. 9. Plot of field against thickness of crust, from values in Table 1 (1 gamma = 1 nanotesla)

of what interpretations we finally make of them, these linear relationships may be regarded as an observational fact. It is shown elsewhere (Hall, 1974) that such linear relationships are to be expected for the model under consideration.

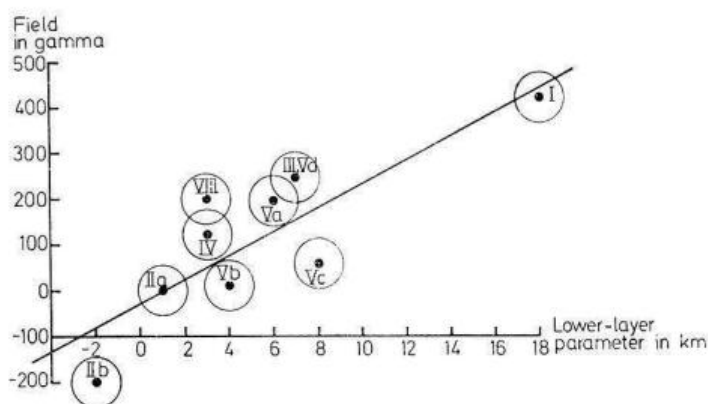


Fig. 10. Plot of field against lower-layer parameter $t = Z - 1.5z$, from values in Table 1 (1 gamma = 1 nanotesla)

Distributions of Magnetization Consistent with the Layered Model

If the R and M discontinuities are boundaries of magnetic zones, then a number of possible configurations might exist, as shown on Fig. 11. These may be summarized as follows.

(1) magnetization lying in the upper crustal layer between some horizon and the R -discontinuity, with magnetization absent (or relatively weak) in the lower crustal layer and upper mantle;

(2) magnetization extending downwards from the R -discontinuity, to a horizon at some level below (in the lower crust or the upper mantle), with magnetization absent (or relatively) weak in the upper crustal layers;

(3) magnetization extending downwards from a horizon at some level, to the M -discontinuity magnetization is absent (or relatively weak) below;

(4) magnetization extending from the M -discontinuity down to a horizon somewhere in the upper mantle. Magnetization is absent (or relatively weak) in the crust;

(5) magnetization extending through the lower crustal layer, and

(6) any of the above cases, but with boundaries of the magnetic zones conformable with the seismic discontinuities rather than coinciding with them.

Analysis of the Linear Plots

It may be shown (Hall, 1974) that for these configurations, F (the field strength) is proportional to either z (depth to Riel), Z (depth to Moho) or a quantity t if the field is caused by a uniformly magnetized lower layer.

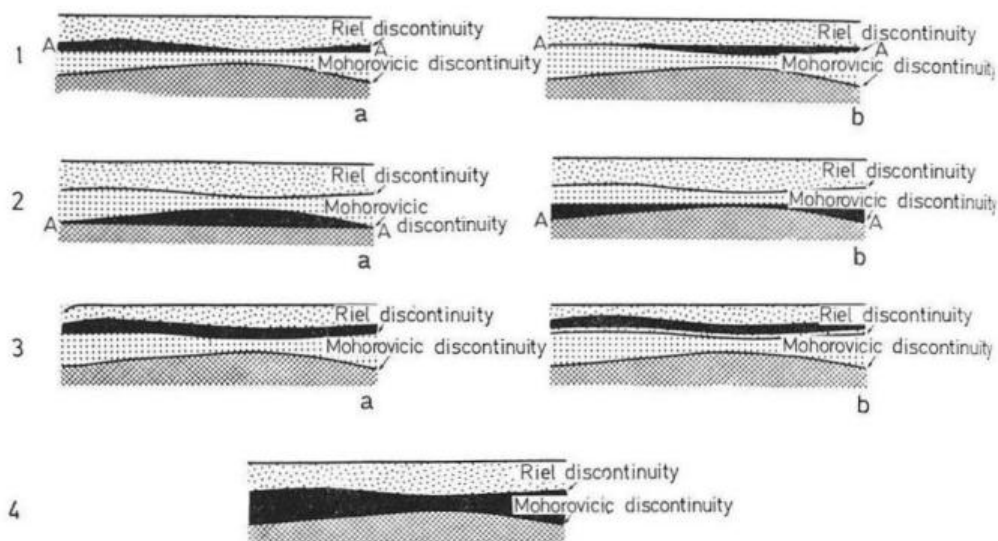


Fig. 11. Ways in which the R and the M discontinuities can control a magnetized zone (in black). Those marked AA have one horizontal surface; those marked "a" lie above. Case 1 is for the R and 2 for the M discontinuity; 3 is for a conformable magnetized zone; 4 is for a magnetic lower crustal layer

The quantity t is called "the lower layer parameter" and is given by $t = Z - 1.5z$ in the area under study. The slopes of the plots of F versus these quantities yield values of the corresponding intensities of magnetization.

Isostatic Case

A possible difficulty arises in using the plots of Figs. 8, 9 and 10 to distinguish the cases outlined in the previous section. If the depths to the R and M discontinuities are everywhere in the area under study related linearly (as would occur for areas related by any one isostatic system (Fig. 13) and if any one of the cases holds, involving control of magnetization by depth to the Riel, or to the Moho or by lower-layer thickness (leading to a linear plot of F versus the appropriate depth or thickness parameter), the plots for the other parameter would also be linear. This circumstance might make it difficult to use these plots to distinguish among the possible cases.

For hydrostatic equilibrium of crust in mantle, given any one isostatic system, we have:

$$z = - \left(\frac{\sigma_3 - \sigma_2}{\sigma_2 - \sigma_1} \right) Z + C \quad (1)$$

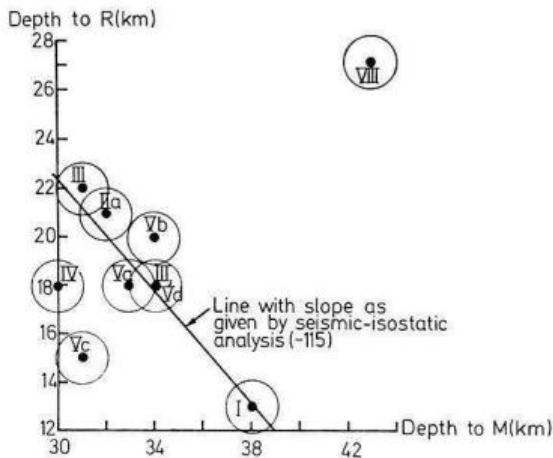


Fig. 12. Isostatic plot for crust in hydrostatic equilibrium with mantle, from values in Table 1

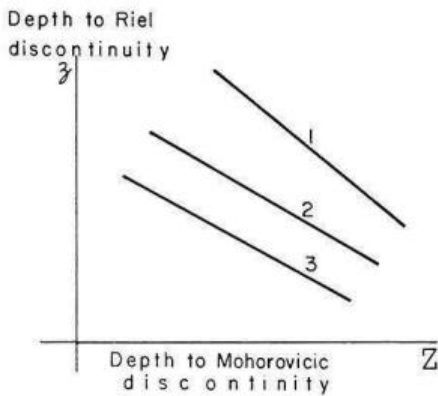


Fig. 13. Isostatic systems in plots such as Fig. 12

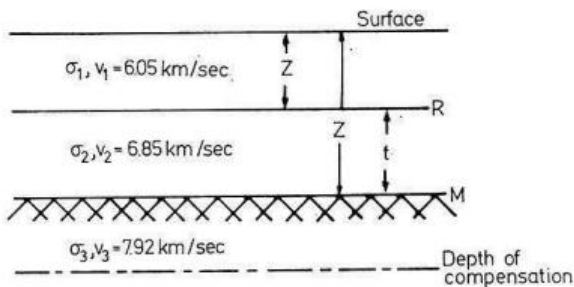


Fig. 14. Airy-Heiskanen model for isostatic plot

where z and Z are depth to Riel and Moho respectively, and C is a constant depending on the densities and the depth of compensation. This equation may be derived for a simple Airy-Heiskanen isostatic model (Fig. 14). Furthermore, in the case where $\sigma = AV + B$ (Birch, 1961, p. 302), with A and B constant over the area, $\sigma_n - \sigma_m = A(V_n - V_m)$. Hence seismic velocities can be used directly in Eq. (1) to determine the multipliers of Z , leading to what has been called the seismic-isostatic method in crustal studies (Hall, 1968b). The velocity values given by Hall and Hajnal (1969, 1973) (all with standard deviations of 0.05 km/sec) give:

$$z = (-1.35 \pm 0.30) Z + C \quad (2)$$

Brown (1968) found these values applicable in detailed studies of isostasy, applying the seismic-isostatic method in conjunction with studies of gravity anomalies over the three southern-most blocks of Fig. 6.

Over an area where the density model down to the level at which compensation takes place, and the depth of compensation, remain constant, a plot of z versus Z forms a single straight line. If any of these conditions differ in an adjacent area, a different line will relate z to Z for that area. Thus these two depths are related in general by families of lines, as shown in Fig. 13. Each line will be referred to as related to a particular "isostatic system".

It is evident that in any isostatic system, z and Z will be proportional. Then if F is related to any one of z , Z , or t by a linear relationship, a plot of F against any other of these quantities will also be linear. Thus plots of F against these depth or thickness parameters would not distinguish one case from another, given a single isostatic system.

Isostatic Systems in the Area

Let us examine isostasy in the area to see if these problems might be encountered in our analysis. In Fig. 12, Riel depth is plotted against Moho depth. It is evident that a single isostatic system holds, by and large, in the area. At first sight this fact would indicate that it will be impossible to use the linear plots to distinguish among the various models considered (Fig. 11). However, Fig. 12 shows some interesting deviations from the system which is obviously dominant over much of the area. These anomalous cases are of importance in evaluating possible magnetic models.

Possible Discrimination between Magnetic Models

Regions IV, Vc and VIII are with the main group of points in Fig. 12. Thus for these three points, the equivalence of the models in Fig. 11 does not hold. If their points in any of Figs. 8, 9, or 10 lies closer to the main

line than in the remaining two plots, then this circumstance can be taken as evidence for favouring the type of magnetization represented by that particular plot. Before we proceed to the selection of our preferred model, let us examine the intensities of magnetization within the crust implied by the various cases represented on Fig. 11. These values are 7.7×10^{-3} emu/cm³ (case 1), 16.6×10^{-3} emu/cm³ (case 2), and 5.4×10^{-3} emu/cm³ (case 4), as derived from the slopes of the plots in Figs. 8, 9, and 10. We should note that the values of these slopes conform within the limits of error given, to the interrelationships given in Eqs. (1) and (2). Thus, as would be expected from Fig. 12, the field versus depth plots are, in their slopes at least, isostatically interrelated.

Selection of Model

Interpretation of Derived Intensities of Magnetization

The method of interpretation used does not require that magnetization be continuously distributed laterally in the layers considered. Linear field versus depth plots would still be possible, as long as a significant portion of each zone of Fig. 6 was underlain by magnetization in the layer under consideration. The linear plot would imply that the intensities of magnetization are roughly the same in all the magnetized portions of the layer and the value of the intensity derived from the slope of the line would be an average of the intensities of these magnetizations.

The derived intensities are 7.7×10^{-3} , 16.6×10^{-3} and 5.4×10^{-3} emu/cm³, depending on whether the M discontinuity, the R discontinuity or the lower-layer thickness are taken as controlling the long-wavelength anomaly field. If we exclude any special conditions at depth acting to enhance the intensity (such as the Hopkinson effect) and consider intensities of magnetization measured for surface samples as a reliable guide, the figures quoted above leave only the last of the three of them as an acceptable possibility. This conclusion follows from what is known about the intensities of magnetization of igneous rocks (of which the crustal layers are most likely largely composed). From intensities as measured on samples, it appears that (excluding very young volcanic rocks) the largest value of J (the sum of induced and remanent intensity) for rocks common enough to be spread over large areas is for basalts. Typical values of J for ocean-floor basalts are in the range $3-5 \times 10^{-3}$ emu/cc. Granitic rocks average one order of magnitude less. Nagata (1961, p. 313) cites values for J for the "granitic" and "basaltic" crustal layers for a locality in Japan as 1×10^{-3} and 5×10^{-3} emu/cm³ respectively as determined from magnetic anomalies.

Recent volcanoes and flows provide interesting results. Averages of J over a whole volcano or system of flows are found up to 50×10^{-3} emu/cm³ (Malahoff, 1969, p. 446). However, the bulk of this magnetization is due to remanence (TRM). This type of magnetization decays with time. If the relaxation time and law of decay suggested by Nagata (1961, p. 155) holds, assuming a Q of 10 (a reasonable value for young volcanic rocks), J would be reduced to below 5×10^{-3} emu/cm³ after 10^9 years. Thus, even if the precambrian crust had originally been built up to a large extent by volcanic processes, incorporating in it rocks with J 's typical of today's young volcanoes and flows, we would expect these intensities to have dropped to the lower values typical of (say) ocean floor basalts.

Discussion of the Particular Models

a) Riel Discontinuity Alone Controlling the Anomalies. If the magnetization were to be above the discontinuity, it would have to be reverse magnetization. The required value (7.7×10^{-3} emu/cm³) would be possible in precambrian rocks only under exceptional circumstances. Reverse magnetization would require a remanent intensity higher than J . The largest values of J reported for magnetic units at depth in the upper crust in the area are about 4×10^{-3} emu/cm³ (Hall, 1968a, p. 1286); also, this magnetization lies in concentrations of limited extent (for example, 30 km wide and 5 km deep, as beneath the Aulneau dome). Surface sampling in the area similarly indicates that values as high as 7.7×10^{-3} emu/cm³ are not encountered over wide areas (Hall, 1968a; Coles, 1973). As regards direction of magnetization, predominantly normal magnetization is suggested for the upper crust (Hall, 1968a) from the interpretation of regional magnetic anomalies, as well as from measurements of remanent magnetization of surface samples (Coles, 1973). Magnetization below the discontinuity would be normal in direction, and remanent and induced intensity of magnetization could be as low as 3.35×10^{-3} emu/cm³ (for $Q = 1$). The value 7.7×10^{-3} emu/cm³ for J is still somewhat higher than values encountered previously in the interpretation of regional magnetic anomalies.

b) Mohorovicic Discontinuity Alone Controlling the Anomalies. This case appears to be ruled out on all reasonable grounds, because of the large intensity (16.6×10^{-3} emu/cm³) required.

c) Magnetized Lower Layer. This case suggests reasonable intensity values; also, it is pointed to as a possible case by a number of other circumstances. First of all, the three points for regions IV, Vc and VIII (which lie off the main Manitoba isostatic model in Fig. 12, and therefore are possible discriminating points in the selection of models) lie closer to the best-fit

line in Fig. 10 than they do in Figs. 8 or 9. This circumstance points to the lower-layer model as the best of the three discussed in the present section. Consequently this model was tested further as described in the section below.

Further Tests of the Lower-Layer Model

Coles (1973) has developed a computer programme (Block) to calculate the field over a system of magnetized blocks, each of which can be assigned values for intensity and direction of magnetization. This programme was used as a further test of our model. The lower crustal layer over the area under study was divided into 70 blocks, each extending vertically through the layer, using depths as given by Figs. 2 and 3. Intensity of magnetization was taken as 5×10^{-3} emu/cm³ and direction of magnetization as parallel to the geomagnetic field. This choice of direction was based on the fact that in earlier deep crustal interpretations (Hall, 1968a, p. 1286 and 1292), near-normal directions of magnetization were found. Subsequently published results of measurements of remanent magnetization of surface rocks in the area (Coles, 1973) support this choice. Contours of the field calculated using Block are shown in Fig. 15. In comparison with Fig. 5 (the long wavelength anomaly map) it can be seen that in general there is good agreement. Some difference in detail is to be expected as the result of lateral inhomogeneities at all levels in the crust. The most serious disagreement occurs at the Bloodvein anomaly, marked as an "anomalous zone" on Fig. 6. The nature of this zone merits a separate discussion.

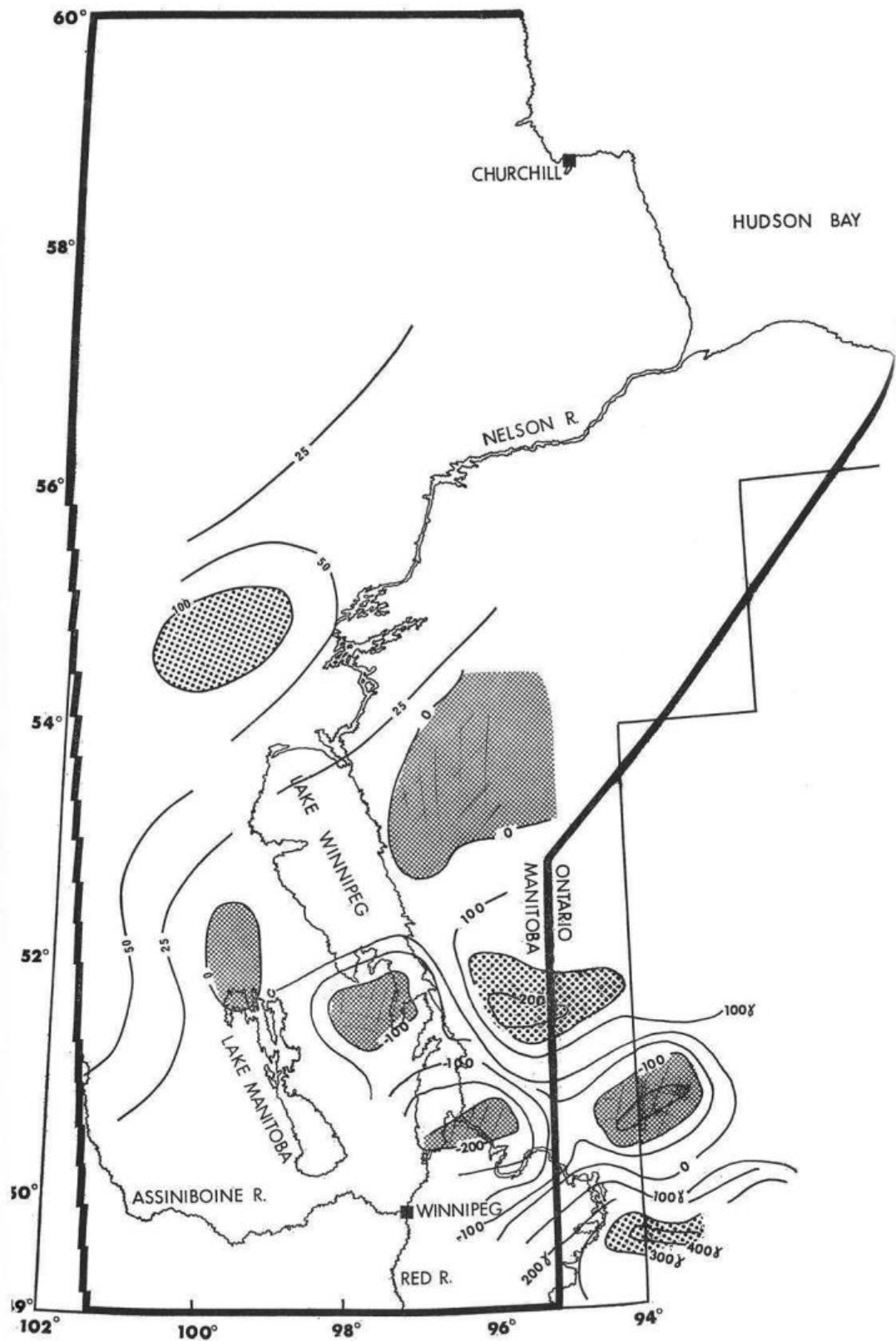
The Bloodvein Anomaly

This anomaly raises two problems. Either it represents a trend in crustal structure which is not correctly represented by the seismic surveys, or it represents a major inhomogeneity above or below the interface between the crustal layers. Application of Hall's (1968c) method of fitting a sloping step to anomaly curves strongly favours a distribution of magnetization lying in the upper crustal layer, for the Bloodvein anomaly. This interpretation would suggest that the long-wavelength anomaly field is not inconsistent with the seismic discontinuities in this locality.

Apart from the reasonable exception of the Bloodvein anomaly, the block-modelling of the lower crust shows the lower-layer interpretation to be an adequate representation of the observed field.

Interpretation in the Frequency Domain

Interpretations of power spectrum versus frequency (Coles, 1973) also show that crustal sources are consistent with the observed data.



Extension beyond the Area of Mapped Riel and Moho

The set of depth-field plots allows extension of our interpretations to several areas beyond that covered by our maps of the R and M discontinuities. A line of recordings of explosions in Lake Superior (during project Early Rise) was run to the north and east of the area by Mereu and Hunter (1969), who interpreted depths to the M -discontinuity from them. These results were compiled with the Manitoba results and with the results of crustal seismic surveys in Hudson Bay by Hall (1971).

Area VI (Table 1 and Fig. 6) lies over Mereu and Hunter's (1969) traverse. Average field and depth to M are known for the area, and are plotted on Fig. 9. Area VI, as can be seen, fits the plot reasonably well. If the layered model can be extended to this area, with the main conclusion of our analysis that magnetization in the lower crustal layer is most likely if the model holds, then we can draw the following conclusion. (1) The area is part of the main Manitoba isostatic system (otherwise, given lower-layer magnetization, there would be no agreement with Fig. 9); (2) The R -discontinuity is present, and its depth is in the 17–19 km range (as is seen by comparing the average field (150 γ) for the area with Fig. 8). If the above calculations and conclusions prove to be correct, we have the basis of a *magnetic-isostatic method* of studying crustal structure.

Area Vd is one of particular interest since it lies almost certainly in the Churchill province of the Canadian Shield. Its position can be viewed as being north of a broad and complex zone separating the Superior and Churchill provinces. Mereu and Hunter's (1969) traverse crosses this area, indicating beneath the traverse a section of considerable thickness (40 km). The area is marked by having field values ranging up to 800 γ (no other area has values in excess of 400 γ). The values of F and depth to M from Table 1 for Area Vd, fit Fig. 9 acceptably. Like Area VI, this area must be part of the main Manitoba isostatic system, and the R -discontinuity must be present. In this case, its depth would be in the 10–12 km range. We might conclude further that the whole of area Vd is underlain by a relatively thick crust.

Another area of interest is the portion of Fig. 5 north of 59° latitude (marked as Area VII on Fig. 6), where the field drops to a relatively low average value, 200 γ . It was indicated in earlier crustal studies of the region (Hall, 1968b, p. 358), that the crustal model of region VIII (the

←

Fig. 15. Component of magnetic field parallel to the geomagnetic field, calculated by programme Block modelling lower crustal layer, assuming uniform magnetization of 5×10^{-3} emu/cm³, parallel to earth's field. Field values are in gammas (1 gamma = 1 nanotesla; $I_{SI} = 4\pi I_{EMU}$)

western portion of Hudson Bay) extends into the area. The field value of 200 γ , agreeing as it does with that for area VIII, is consistent with this hypothesis. This area lies over an important structural element of the Churchill geological province, the Wollaston Lake fold belt (see e.g. Davidson, 1972, p. 388). Our geophysical analysis indicates this structure as being characterized by a relatively thick crust, a relatively thin lower layer and a moderate to low long-wavelength magnetic anomaly field.

These additional cases add strength to the hypothesis of lower-layer magnetization, since they exhibit markedly different conditions all conforming with one aspect or another of the layered model.

Lateral Inhomogeneities

The alternative remains that some or even all of the features on Fig. 5 could be explained by lateral concentrations of magnetization. These could be relatively thin near-surface plates, or concentrations at greater depths within the crust. Let us examine some possible cases.

Deep Distributions

It is of considerable importance to examine lateral concentrations of magnetization as possible explanations of the field difference between Areas Ib and IIb. This point is critical because the points for Areas I and IIb are key ones in establishing the linearity of the plots in Figs. 7–10.

All indications point to near-normal magnetization in the crust in the area. This case was, therefore, investigated by examining the effect of a block of magnetization lying beneath the large anomaly with 600 γ peak (Fig. 5), in Area Ib, contrasted with no magnetization anywhere beneath Area IIb. The amplitude of the anomaly could be reproduced by a block extending vertically through the upper crust, with intensity of magnetization equal to 3×10^{-3} emu/cm³. Or, it could be reproduced by a block extending downwards through the lower crust, with an intensity of 5×10^{-3} emu/cm³. On the basis of the required intensity values, both possibilities are reasonable. However, the block in the lower crust reproduces the anomaly shape better than does the one for the upper crust. It is in fact the best-fit block. Thus a deep crustal distribution is a reasonable one as an explanation of the anomaly, with the result pointing towards a lower-crustal source. This latter model (lower-crustal block) would in fact fit the long-wavelength anomaly field reasonably well. Thus, if lower-crustal magnetization is present, it could be either continuously or discontinuously distributed laterally in the layer. An argument in favour of an upper-crustal source might be the fact that a lower intensity is required, although the required intensity in the lower layer is not unreasonable for basalt.

Thin Near Surface Plate

If a relatively thin near-surface block is considered as the source of the anomaly in zone Ib, it is found that an intensity of 6×10^{-3} emu/cm³ is required for a thickness of 5 km. Thus an exclusively near-surface source of the anomaly appears to be unlikely because of the high values of intensity required. A similar argument applies to zone Vb.

Final Choice of Magnetic Model

It would appear that there is a good case for the hypothesis that over the area treated, there is widespread deep crustal magnetization giving rise to the long-wavelength anomaly field. The most likely location of this magnetization is in the lower crustal layer, although the interpretations made to date leave also the upper crust as a possible location for it. The inferred intensity of magnetization lies within common ranges found for basalts, other than the very youngest. There is a rather interesting connection between these results, deduced from the long-wavelength anomalies, and previous results (Hall, 1968a) from intermediate-wavelength anomalies. In the latter case, zones of magnetization, some tens of kilometers across, and of vertical dimensions extending from an average of 7 km below the surface to an average of 17 km depth were found. These zones appear to lie beneath granitic plutons, common in the area. The magnetic zones at depth beneath these granitic areas have an intensity of magnetization averaging 3×10^{-3} emu/cc. These zones may represent lower-layer material rising behind the granite plutons during their emplacement (or the residue in a differentiation process), or simply a physical zoning, where upwelling heat favoured the generation of magnetic minerals. Thus these zones in the upper crustal layer would appear to be in some way connected with the lower layer. These relationships are sketched in Fig. 16.

In an earlier interpretation Hall (1968a) examined the evidence offered by the data then available on the presence or absence of lower-layer magnetization. He suggested that, although a definite conclusion was not yet possible, that it appeared that lower-layer magnetization was absent. It is now clear, after considerable extension of the coverage, that the initial area was not suited to revealing the deeper magnetization, and that the subsequent coverage suggests this deeper component.

Conclusions

In the present paper, a new type of magnetic anomaly map for Manitoba and northwestern Ontario (filtered aeromagnetic anomalies in the range of anomaly width $60 \text{ km} < \lambda < 4000 \text{ km}$) is presented. This map

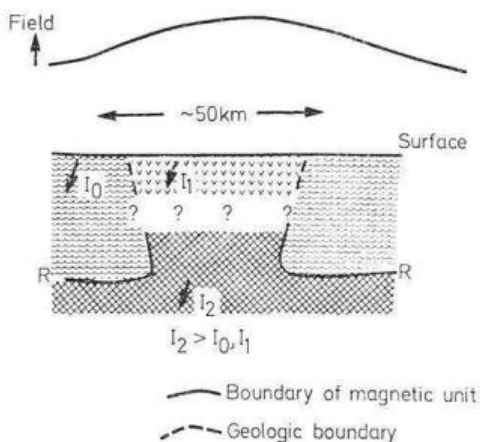


Fig. 16. Suggested distribution of magnetization below granitic areas where regional anomaly highs occur, combining magnetic units treated by Hall (1968a) and results of the present paper

shows close correlation with deep crustal structure as mapped by seismic sounding. This correlation takes the form of straight-line relationships between the field and the following quantities: depth to boundary between upper and lower crustal layers; total thickness of crust, and thickness of lower crustal layers. The plausibility of lateral inhomogeneities being the cause of the anomalies was also investigated, using block models. In addition, the effect of isostatic compensation on results derived from crustal layering was considered. The following conclusions emerged.

(1) Most of the areas within the region fall within a single isostatic system. Three regions do not. If all regions fall within one system, it is impossible to discriminate among the three possibilities for layered models mentioned above. If some regions do not, discrimination is possible.

(2) There are anomalous regions, however, and these point to the lower crustal layer as the most probable seat of the origin of the long-wavelength anomaly field. The required intensity of magnetization in this layer would be 5.3×10^{-3} emu/cm³; this value is close to the average value for measured samples of basalt.

(3) The upper crustal layer is also a possible seat for magnetization related to the long-wavelength anomaly field, although the lower layer is more probable on the basis of the data analyzed in the present paper.

(4) Shallow plates of magnetization appear to be very unlikely as the origin of the anomalies. Thus we are led to look for *deep crustal magnetization* whether it lies in the upper or the lower crustal layer.

Acknowledgements. This research was done with support by the National Research Council of Canada, and the University of Manitoba Northern Studies Committee. This support is gratefully acknowledged.

The author wishes to thank Dr. Richard Coles for providing his programme Block for use prior to its publication. The help of Mr. David Richards in computer processing throughout the investigation is acknowledged. Mr. Charles Hasselfield carried out computer processing and programming during the testing of the block models.

References

- Bhattacharyya, B. K., Morley, L. W.: The delineation of deep crustal magnetic bodies from total field aeromagnetic anomalies. *J. Geomagnet. Geoelectr.* 17, 237–252, 1965
- Birch, F.: Composition of the Earth's Mantle: in *The Earth Today*; Royal Astronomical Society. 295–311, 1961
- Brown, R. J.: Isostasy and crustal structure in the English River gneissic belt: Unpublished M. Sc. Thesis. University of Manitoba, 1968
- Coles, R. L.: Relationships between measured rock magnetizations and interpretations of longer wavelength anomalies in the Superior province of the Canadian Shield. Unpublished Ph. D. thesis, University of Manitoba, 215 p., 1973
- Davidson, A.: The Churchill Province: in *Variations in Tectonic Styles in Canada*, 382–388, 1972
- Dominion Observatories Branch: F-isodynamic chart, Canada, 1965
- Hajnal, Z.: A two-layer model for the earth's crust under Hudson Bay; In *Earth Science Symposium on Hudson Bay*, P. J. Hood (ed.) Geological Survey of Canada paper 326–336, 1969
- Hall, D. H., Dagley, P.: Regional magnetic anomalies; An analysis of the Smoothed Aeromagnetic Map of Great Britain and Northern Ireland. Institute of Geological Sciences, Report 70/10, 1970
- Hall, D. H.: Regional magnetic anomalies, magnetic units, and crustal structure in the Kenora District of Ontario. *Can. J. Earth Sci.* 5, 1277–1298, 1968a
- Hall, D. H.: A seismic-isostatic analysis of crustal data from Hudson Bay, in *Earth Science Symposium on Hudson Bay*, P. J. Hood, Ed. Geological Survey of Canada Paper 68–53, 337–364, 1968b
- Hall, D. H.: A magnetic interpretation method for calculating body parameters for buried sloping steps and thick sheets. *Geoexploration.* 6, 187–206, 1968c
- Hall, D. H.: Geophysical determination of deep crustal structure in Manitoba. The Geological Association of Canada, Special Paper No. 9, 83–88, 1971
- Hall, D. H.: In preparation 1974
- Hall, D. H., Hajnal, Z.: Crustal Structure of northwestern Ontario. *Refraction seismology.* *Can. J. Earth Sci.* 6, 81–99, 1969
- Hall, D. H., Hajnal, Z.: Deep seismic crustal studies in Manitoba. *Bulletin of the Seismological Society of America* 63, 885–910, 1973
- Hall, D. H., McGrath, P. H., Richards, D. J.: Regional Magnetic anomalies in Manitoba. Manitoba Mines Branch (in press), 1974
- Malahoff, A.: Magnetic Studies over Volcanoes. Hawaii Institute of Geophysics Contribution 198, 436–446, 1969
- McGrath, P. H., Hall, D. H.: Crustal structures in northwestern Ontario: Regional magnetic anomalies. *Can. J. Earth Sci.* 6, 101–107, 1969

- Mereu, R.F., Hunter, J.A.: Crustal and upper mantle structure under the Canadian Shield from Project Early Rise. *Bull. Seism. Soc. Am.* 59, 147–165, 1969
- Morley, L.W., MacLaren, A.: Magnetic anomaly map of Canada. Map number 1255A, 1967
- Nagata, T.: *Rock Magnetism*, Revised Edition, 350 pp., Tokyo: Maruzen Co., 1961
- Regan, R.D.: World Wide Magnetic Anomalies from Pogo and Cosmos Data, IAGA Second General Scientific Assembly, 1974
- Wilson, H.D.B.: The Superior Province in the Precambrian of Manitoba. *The Geological Association of Canada, Special Paper, No. 9*, 41–49, 1971
- Zietz, I., Andreasen, G.E., Cain, J.C.: Magnetic anomalies from satellite magnetometer. *J. Geophys. Res.* 75, 4007–4017, 1970

D. H. Hall
Geophysics Section
Department of Earth Sciences
University of Manitoba
Winnipeg, Canada